

# A GENERALIZATION OF BEM METHOD APPLIED TO HYDROKINETIC TURBINE DESIGN OF FREE FLOW

**Déborah Aline Tavares Dias do Rio Vaz** – deborah.rio@gmail.com

Universidade Federal do Pará, Faculdade de Engenharia Mecânica

**Claudio José Cavalcante Blanco** – blanco@ufpa.br

Universidade Federal do Pará, Faculdade de Engenharia Sanitária e Ambiental

**Jerson Rogério Pinheiro Vaz** – jerson@ufpa.br

**André Luiz Amarante Mesquita** – andream@ufpa.br

Universidade Federal do Pará, Faculdade de Engenharia Mecânica

**João Tavares Pinho** – jtpinho@ufpa.br

Universidade Federal do Pará, Faculdade de Engenharia Elétrica

**Abstract.** A mathematical model is presented in this work, corresponding to an extension of the classical Blade Element Momentum – BEM theory for the hydrokinetic turbine design with extended operation for tip-speed-ratio less than 2, which is considered the influence of the wake on the rotor plane in the general form. This influence shows considerably when the tip-speed-ratio is small, justifying the development of formulations that predict the effects of the wake on the rotor plane. The proposed mathematical model uses the Glauert's theory, on which to impose a modification and are compared with the results obtained by Sale et al.

**Keywords:** Hydrokinetic rotors, BEM method, Glauert's model.

## 1. INTRODUCTION

The study of mathematical models applied to hydrokinetic rotor design has become prominent for the use of technologies for power generation with low environmental impact. Such models are based generally on the BEM method, considering the induction factor in the wake of the double-inducing factor in the rotor plane (Hansen, 2000) ignoring the generally relationship established by Wilson and Lissaman (1987) for influence of the vortex wake. In the region of slower operation of the turbine, the proposed model, besides in the general form for the axial induction factor in the rotor plane and in the wake, corrects the high values of the induction factor in terms of a modification on the empirical Glauert (1926) relationship. For the correction of the finite number of blades, uses the Prandtl's model (Hibbs and Radkey, 1981). Finally, the results are shown using the model, compared with the classical BEM method (Hansen, 2000) and the model used by Sale et al (2009), which is also based on the BEM method.

## 2. THE MATHEMATICAL MODEL

A flow model that considers the complete equations of angular momentum for rotation in the wake was presented by Joukowski (1918) applied by Glauert (1926) in the study of propulsion, and later modified by Lissaman and Wilson (1974) for the case of wind rotors, where the induction in the flow caused by the mat is twice induction in the rotor plane. Figure 1 shows the flow in a streamtube (Hansen, 2000).

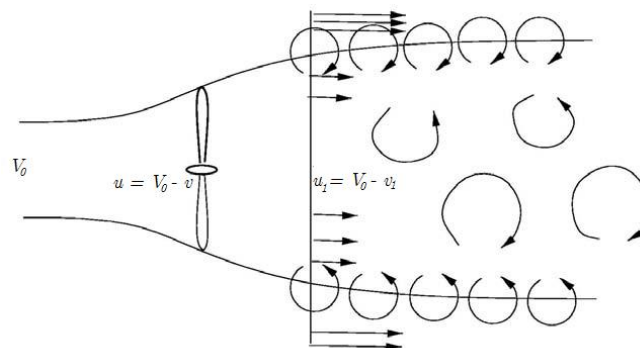


Figure 1. Simplified schematic of the velocities in the rotor plane and wake (Hansen, 2000).

where  $V_0$  is the velocity undisturbed flow. In dimensional terms, the kinetic power is converted into mechanical power by the turbine is given by (Junior Brazil, 2006):

$$E_c = \frac{1}{2} \rho A V_0^3 \quad (1)$$

where  $\rho$  is the fluid density and  $A$  is the area swept by the rotor blades. The velocities  $u$  and  $u_1$  in the rotor plane and wake, respectively, are induced and written in the form:

$$\begin{cases} V_0 - v = u \equiv (1 - a)V_0 \\ V_0 - v_1 = u_1 \equiv (1 - b)V_0 \end{cases} \quad (2)$$

where  $v = aV_0$  e  $v_1 = bV_0$ .  $a$  and  $b$  are the axial induction factors in the rotor plane and wake, respectively.  $X$  is the tip-speed-ratio. Applying the energy equation (Eggleston and Stoddard, 1987) for the induced velocity (Eq. 2), has

$$a = \frac{b}{2} \left[ 1 - \frac{b^2(1-a)}{4X^2(b-a)} \right] \quad (3)$$

The present work assumes that the induction factor  $b'$  has a similar relationship with  $a'$ , which leads to a more general form than that one proposed by Mesquita and Alves (2000).

$$a' = \frac{b'}{2} \left[ 1 - \frac{b'^2(1-a')}{4X^2(b'-a')} \right] \quad (4)$$

$a'$  and  $b'$  are the induction factors in the tangential rotor plane and wake, respectively. To solve Eqs. (3) and (4), it uses Newton's method through Eqs. (5) and (6).

$$\Phi(b) = \frac{b}{2} \left[ 1 - \frac{b^2(1-a)}{4X^2(b-a)} \right] - a \quad (5)$$

$$\Gamma(b') = \frac{b'}{2} \left[ 1 - \frac{b'^2(1-a')}{4X^2(b'-a')} \right] - a' \quad (6)$$

whose iterative solution is obtained by Eqs. (7) and (8). In this case, a good approximation for the start of the iterative process corresponds  $b = 2a$  e  $b' = 2a'$ .

$$b_i = b_{i-1} - \frac{\Phi(b_{i-1})}{\frac{d\Phi(b_{i-1})}{db}} \quad (7)$$

$$b'_i = b'_{i-1} - \frac{\Phi(b'_{i-1})}{\frac{d\Phi(b'_{i-1})}{db'}} \quad (8)$$

The use of Newton's method is to always get the lowest real value for the calculation of  $b$  e  $b'$ , since the variation of induction factors on the wake is completely non-linear in relation to the induction factors in the rotor plane (Fig. 2).

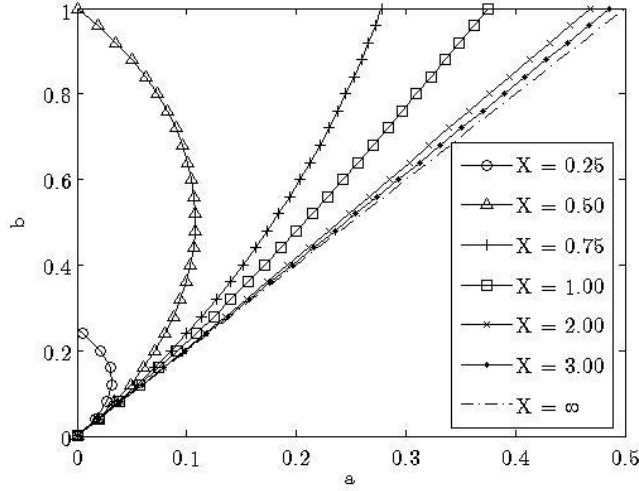


Figure 2. Relationship  $b/a$  for some values of  $X$  (Lissaman and Wilson, 1974).

### 2.1. The Correction for the Glauert's model

From the correlation presented in the work of Hansen (2000), in which the fit of experimental data developed by Glauert (1926) result in

$$C_T = \begin{cases} 4a(1-a)F & a \leq \frac{1}{3} \\ 4a \left[ 1 - \frac{a}{4}(5-3a) \right] F & a > \frac{1}{3} \end{cases} \quad (9)$$

where  $C_T$  is the thrust coefficient and  $F$  is the Prandtl factor. Thus, developing a correction in Eq. (9), in order to consider the general case for calculating the induction factor in the rotor plane, Eq. (3), where the thrust coefficient is dependent of induction factor on the wake. Therefore,  $C_T$  takes the following modified expressions:

$$C_T = \begin{cases} 2b(1-a)F & a \leq \frac{1}{3} \\ 2b \left[ 1 - \frac{a}{4}(5-3a) \right] F & a > \frac{1}{3} \end{cases} \quad (10)$$

The behavior of trust coefficient  $C_T$  as function of  $a$  is shown in Fig. 3, where an increase of  $C_T$  occurs for values of  $X = (1.0, 1.5, 2.0)$ , which is predicted by the relationship between  $b$  and  $a$ , where  $b$  assumes values greater than twice  $a$ , resulting in an increase of values of  $C_T$  for  $a$  around 0.5, since  $C_T$  is directly proportional to  $b$ .

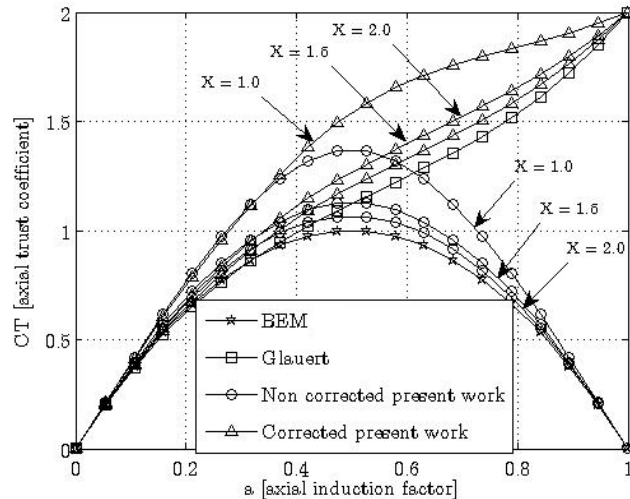


Figure 3. Solutions for the proposed model, BEM and Glauert's methods for some values of  $X$ .

The scheme, using the most general form for the axial induction factor, converges to the classical BEM method, both with and without the correction of Glauert (1926), where  $X$  is greater than 2, (see Fig. 3). Fig. 4 compares the results with experimental data (obtained from Moriarty PJ, Hansen (2005)) for  $X = 4$ , showing good agreement.

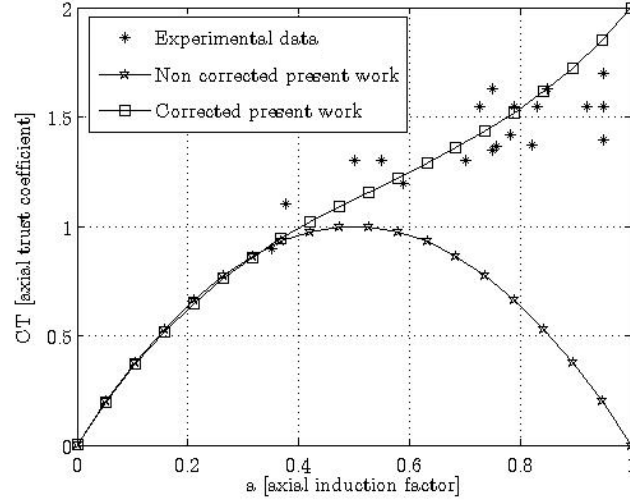


Figure 4. Comparison between proposed model and experimental data for  $X = 4$ .

Equation (10) shows that to  $a > \frac{1}{3}$  the thrust coefficient is fixed, taking into account the values of  $b$ . Since the thrust coefficient in the rotor plane is given by Hansen (2000),:

$$C_T = (1 - a)^2 \frac{\sigma C_n}{\sin^2 \phi} \quad (11)$$

with

$$\sigma = \frac{cB}{2\pi r} \quad (12)$$

and

$$C_n = C_L \cos \phi + C_D \sin \phi \quad (13)$$

where  $B$  is the number of blade,  $c$  is the chord,  $r$  is the local radius,  $F$  Prandtl's correction,  $C_L$  and  $C_D$  are the lift and drag coefficients, respectively,  $\phi$  is the angle of flow.

Equating Eqs. (10) and (11), has:

$$a = \begin{cases} 1 - \frac{2bF \sin^2 \phi}{\sigma C_n}; & a \leq \frac{1}{3} \\ \frac{8 - 5k - \sqrt{k(32 - 23k)}}{2(4 - 3k)}; & a > \frac{1}{3} \end{cases} \quad (14)$$

with

$$k = \frac{2bF \sin^2 \phi}{\sigma C_n} \quad (15)$$

$$\phi = \tan^{-1} \left[ \frac{V_0 (1 - a)}{\Omega r (1 + a')} \right] \quad (16)$$

where  $\Omega$  is the angular velocity. For the calculation of  $a'$ , has

$$a' = \frac{2b'F \sin \phi \cos \phi}{\sigma C_t} - 1 \quad (17)$$

where

$$C_t = C_l \sin \phi - C_d \cos \phi \quad (18)$$

Equation (19) can be obtained at work Alves and Mesquita (2000). For the Prandtl's correction (described by Hibbs and Radkey, 1981), we have:

$$F = \frac{2}{\pi} \cos^{-1}(e^{-f}) \quad (19)$$

with

$$f = \frac{B}{2} \cdot \frac{(R-r)}{r \sin \phi} \quad (20)$$

The iterative procedure for the calculation of induction factors considered known parameters  $r$ ,  $c(r)$ ,  $\beta(r)$ ,  $C_L(\alpha)$ ,  $C_D(\alpha)$  and  $V_0$  as follows:

- (i) Attribute initial values for  $a$  and  $a'$ . In this paper  $a = 1/3$  and  $a' = 0.001$ ;
- (ii) Compute  $b$  and  $b'$  with Eqs. (7) and (8);
- (iii) Compute the value of  $\phi$  to Eq. (16);
- (iv) Obtain  $C_L$  and  $C_D$  from  $\alpha = \phi - \beta$ .  $\alpha$  is the angle of attack and the twist angle  $\beta$ ;
- (v) Compute  $a$  and  $a'$ , by applying Newton's method in Eqs. (14) and (17), making

$$\Psi(a) = -a + 1 - \frac{2bF \sin^2 \phi}{\sigma C_n}$$

$$\Pi(a') = -a' - 1 + \frac{2b'F \sin \phi \cos \phi}{\sigma C_t}$$

since the induction factors depend on the heels of induction factors in the plane of the rotor,  $b = b(a)$  and  $b' = b'(a')$ , so

$$a_i = a_{i-1} - \frac{\Psi(a_{i-1})}{\frac{d\Psi(a_{i-1})}{da}}$$

$$a'_i = a'_{i-1} - \frac{\Pi(a'_{i-1})}{\frac{d\Pi(a'_{i-1})}{da'}}$$

- (vi) Applies the Glauert's model modified, Eq. (14);
- (vii) Verify the convergence for  $a$  and  $a'$ . If the tolerance is not achieved, return to (ii). In this work, tolerance is considered  $10^{-3}$ .

The power coefficient  $C_p$  is given by Mesquita and Alves (2000), by Eq. (21).

$$C_p = \frac{4}{X^2} \int_0^X (1 - aF) F b' x^3 dx \quad (21)$$

The power output of the turbine is

$$P = \frac{1}{2} C_p \rho A V_0^3 \quad (22)$$

### 3. MODEL FOR POST-STALL CORRECTION

According to Alves (1997), the quality of results obtained from models based on the BEM method, depends heavily on an accurate of the characteristics of lift and drag of the blade, which, for small angles of attack before stall are well established, theoretically and experimentally. Lissaman (1994) shows that the region where the boundary layer remains affixed is usually restricted to angles of attack more or less  $15^\circ$ , while, during the operation of a rotor, the airfoil can try angles of attack much higher, entering the zone in which any separation of the boundary layer (up to  $30^\circ$ ), or even experiencing the system completely apart, between  $30^\circ$  and  $90^\circ$ , where usually do not know the characteristics of lift and drag. Lissaman (1994) developed these studies for the case of wind turbines. In this work, such studies are extended to the case of disposal of water to adjust the hydrokinetic turbine.

The aspects mentioned above are important in predicting the maximum power developed by a rotor fixed blades (vital for a safe design of the power system) on the occurrence of strong velocity when large part of the blade experiences high angles of attack. The non-inclusion of these effects leads to a underestimation of maximum power. So Viterna and Corrigan (1981) proposed an empirical model for change the airfoil in all three regimes of operation in order to more accurately forecast the behavior of a rotor axis. When the angle of attack is equal to or higher than that at the beginning separation, the model Viterna and Corrigan (1981) provides the following values for drag and lift coefficients:

$$\alpha \geq \alpha_{\text{separation}} :$$

$$C_l = \frac{C_{d,\text{max}}}{2} \sin 2\alpha + K_l \frac{\cos^2 \alpha}{\sin \alpha} \quad (5)$$

$$C_d = C_{d,\text{max}} \sin^2 \alpha + K_d \cos \alpha \quad (6)$$

$$K_l = (C_{l,s} - C_{d,\text{max}} \sin \alpha_s \cos \alpha_s) \frac{\sin \alpha_s}{\cos^2 \alpha_s} \quad (7)$$

$$K_d = \frac{C_{d,s} - C_{d,\text{max}} \sin^2 \alpha_s}{\cos \alpha_s} \quad (8)$$

$$\mu \leq 50: \quad C_{d,\text{max}} = 1,11 + 0,018\mu \quad (9)$$

$$\mu > 50: \quad C_{d,\text{max}} = 2,01 \quad (10)$$

$$\mu = \frac{R - r_{\text{cub.}}}{c(r)}$$

where  $C_{d,\text{max}}$  is the maximum drag coefficient in the region completely separate. Viterna and Corrigan (1981) model is appropriate since, that this model gives good results for the NACA profiles (Abbot and Doenhoff, 1959 and Alves, 1997). Figure 5 shows the lift and drag coefficients corresponding to the NACA 4418 profile (Abbot and Doenhoff, 1959) used in this work. The Reynolds number used in the simulation is  $3 \cdot 10^6$ .

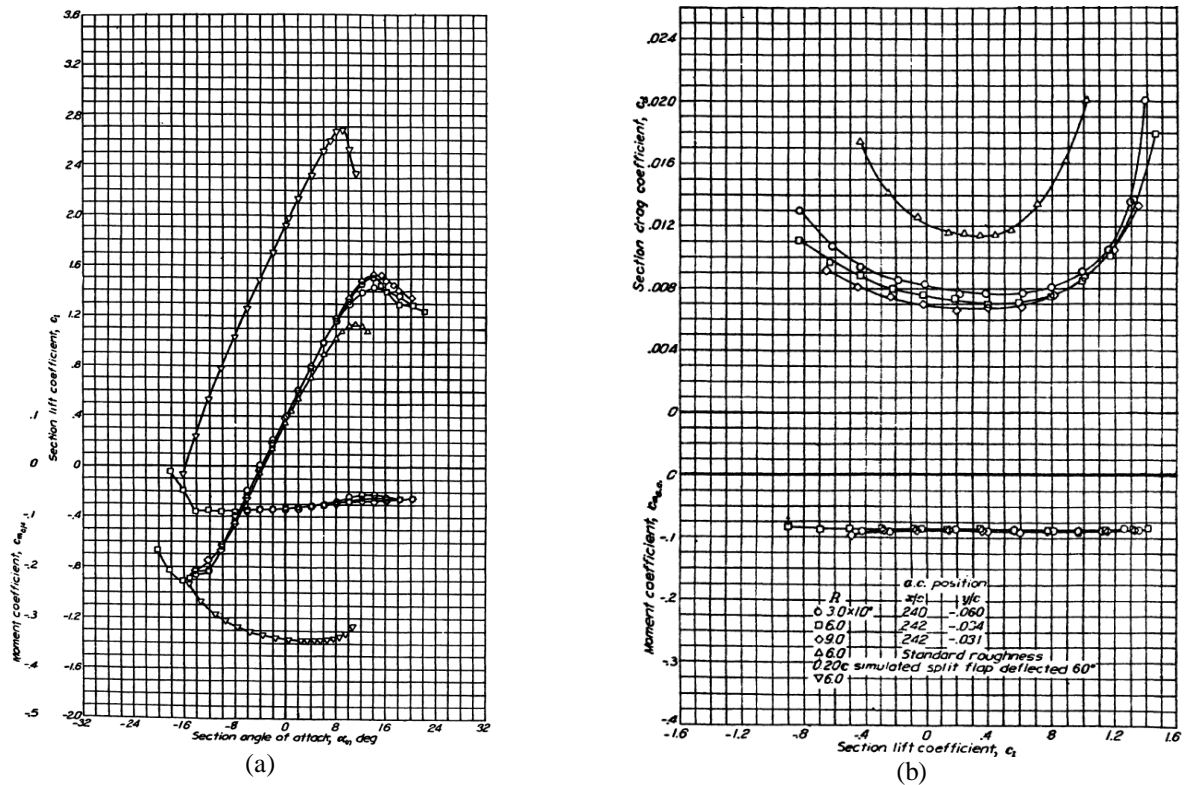


Figure 5. (a) Lift coefficient in relation to the angle of attack for the NACA 4418 profile. (B) Drag coefficient in relation to the lift coefficient for NACA 4418 profile.

#### 4. COMPARISON WITH OTHER MATHEMATICAL MODELS

The models for comparison are: WT\_Perf developed by National Wind Technology Center's current used by the National Renewable Energy Laboratory - NREL WT\_Perf that extended to the hydrokinetic turbines design (Sale et al, 2009) and classical BEM model shown in detail in the work of Hansen (2000). The hydrokinetic turbine is Verdant Power (Fig. 6) without diffuser, with rate power of 35 kW, regulated by stall, diameter 5 m, 3 blades, rotation 28 rpm.



Figure 6. Hydrokinetic Turbine Verdant Power 35kW (Sale et al, 2009).

The turbine blades were obtained using a combination of airfoil NACA 44XX series by NREL (Sale et al, 2009). In this work are considered the lift and drag coefficient for the NACA 4418 (Abbot and Doenhoff, 1959) used for model validation. Figs. 7 and 8 show the comparison between the results obtained, considering the stall for angles of attack equal or greater than  $15^\circ$ . It is observed in Fig. 7 is a substantial difference to the power coefficient in velocity range

between 0.7 and 1.4 m/s. This difference is mitigated in the calculation of rotor power output (Fig. 8), since the power varies with the cube of water velocity, which causes the energy generated by the turbine is small for low values of velocity, according to the comparison shown in Fig. 8. This figure shows that the output power is more sensitive to variations of power coefficient to higher values of velocity, as occurs in the range between 1.7 and 2.5 m/s (Fig. 8).

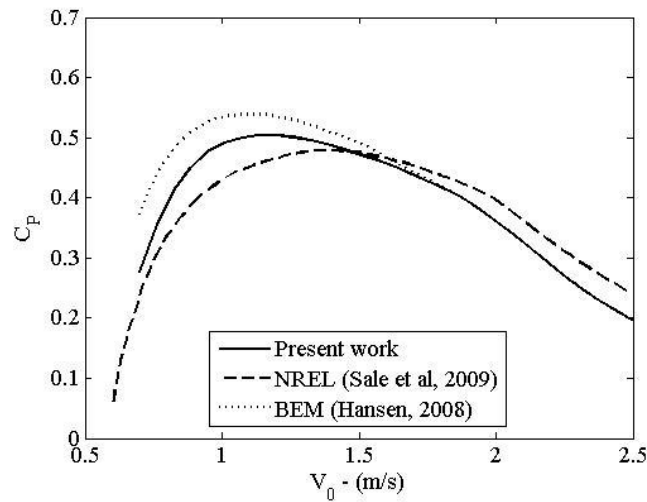


Figure 7. Power coefficient vs. flow velocity with corrections at angles of attack equal or greater than 15°.

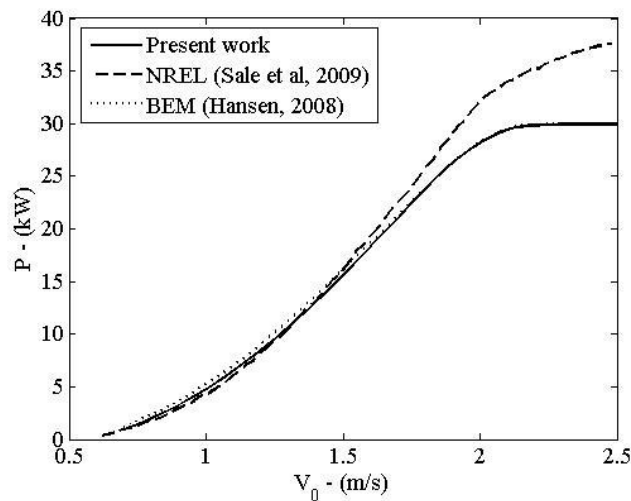


Figure 8. Mechanical power vs. flow velocity with corrections at angles of attack equal or greater than 15°.

Figures 9 and 10 show the results obtained without Viterna and Corrigan correction. As in Fig. 7, the difference in the power coefficient is attenuated in the calculation power curve in the same range of flow velocity. For the velocity range between 1.5 and 2.5 m/s occurs considerable improvement compared with the results obtained by Sale et al (2009). Figure 10 confirms the good result for the power curve, where the proximity of the curve obtained using the proposed model with the curve simulated in the work of Sale et al (2009) is appreciable.



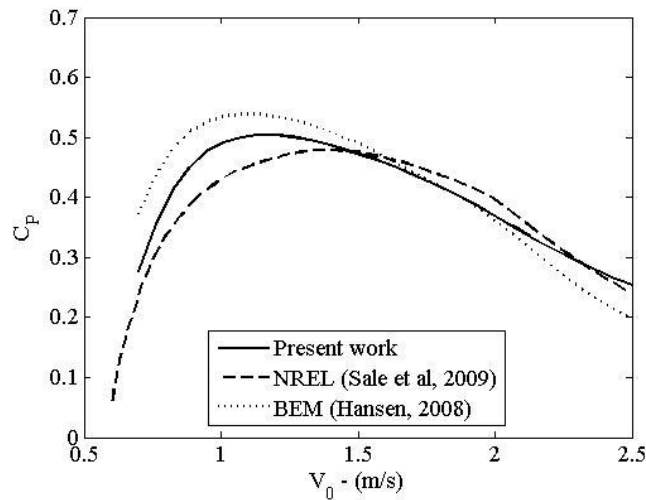


Figure 9. Power coefficient vs. flow velocity without Viterna and Corrigan correction.

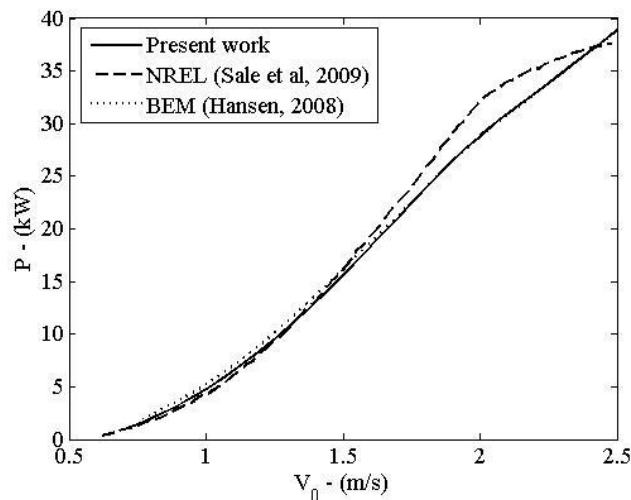


Figure 10. Mechanical power vs. flow velocity without Viterna and Corrigan correction.

The distance between the curves in part has to do with the aerodynamic shape of the blades, once the rotor Verdant Power was built using a set of profiles along the radius, based on NACA 44XX series, the set of profiles was omitted in the work of Sale et al (2009). In this paper, the simulation was developed using single profile along the blade (NACA 4418), which shows good approximation.

## 5. CONCLUSION

The mathematical model presented in this work represents an alternative tool for the rotors hydrokinetic design for free flow, where the main advantage of the model is that in its main structure is pre-order the equation more that relates the general induction factors in the rotor plane and in the wake established by Wilson and Lissaman (1987). The model also considers the Glauert (1926) correction, that has been modified in order to meet the conditions set by Eqs. (3) and (4). The comparisons show that the developed model shows good agreement when compared with the model of NREL (Sale et al, 2009) and the classical BEM method (Hansen, 2000). It is noted also that the model shows good efficiency, especially for low speeds flow, common in rivers of the Amazon. This model can be extended to the rotors with a diffuser and to better the efficiency of the turbine.

## 6. ACKNOWLEDGMENTS

This work was developed in the Grupo de Estudo e desenvolvimento de Alternativas Energéticas - GEDAE, member of the Instituto Nacional de Ciência e Tecnologia de Energias Renováveis e Eficiência Energética da Amazônia - INCT - EREEA as part of a project funded by Conselho Nacional de Desenvolvimento Científico e Tecnológico - CNPq.

## 7. REFERENCES

- Abbot, J. H. and Doenhoff, V., 1959. *Theory of Wing Suctions*, *Dover Publications Inc*, 2<sup>nd</sup>. Edition.
- Alves, A. S. G. , 1997. Análise do Desempenho de Rotores Eólicos de Eixo Horizontal, *Dissertação de Mestrado*, Universidade Federal do Pará, Brasil.
- Brasil-Junior, A. C. P., Salomon, L. R. B., Els, R. V., Ferreira, W. O., 2006. A New Conception of Hydrokinetic Turbine of Isolated Communities in Amazon, IV Congresso Nacional de Engenharia Mecânica, Recife, Pernambuco, Brasil.
- Eggleston, D. M. and Stoddard, F. S., 1987. “Wind Turbine Engineering Design”, Van Nostrand Reinhold Company, New York.
- Glauert H., 1926. *The elements of airfoil and airscrew theory*. Cambridge: Cambridge University Press.
- Hansen, M., “Aerodynamics of Wind Turbines”, 2<sup>nd</sup> Edition, Earthscan, 2008.
- Hansen MOL. Documentation of code and airfoil data used for the NREL 10-m wind turbine. ROTABEMDTU, November 2000.
- Hibbs, B., Radkey, R. L., 1981. Small Wind Energy Conversion System Rotor Performance Model Comparison Study. Rockwell Int. Rocky Flats Plant, RFP-4074/13470/36331/81-0.
- Joukowski, N. E., 1918. *Travanx du Bureau des Calculs et Essais Aeronautiques de l’Ecole Superieure Technique de Moscou*.
- Lissaman, P. B. S., 1994. Wind Turbine Airfoils and Rotor Wakes, in Spera, D. A. *Wind Turbine Technology*, ASME Press. Cap. 6.
- Mesquita, A. L. A. and Alves, A. S. G., 2000. An Improved Approach for Performance Prediction of HAWT Using Strip Theory, *Wind Engineering*, Vol. 24, No. 6.
- Moriarty PJ, Hansen AC, 2005. AeroDyn theory manual. Technical report NREL/TP-500-36881—January.
- Ostowari, C., and Naik, D., 1984. Post-Stall Wind Turbine Studies of Varying Aspect Ratio Wind Tunnel Blades with NACA 44XX Series Airfoil Sections, Golden, Colorado: *National Renewable Energy Laboratory*.
- Sale, D., Jonkman, J., Musial, W., 2009. Hydrodynamic Optimization Method and Design Code for Stall-Regulated Hydrokinetic Turbine Rotors. ASME 28th International Conference on Ocean, Offshore, and Arctic Engineering Honolulu, Hawaii May 31–June 5.
- Vaz, J. R. P., Silva, D. O., Mesquita, A. A, Lins, E. F., Pinho, J. T., 2009a. Aerodynamic and Modal Analyses of Blades for Small Wind Turbines, 20th International Congress of Mechanical Engineering, Gramado, Rio Grande do Sul, Brazil.
- Viterna, L. A., and Corrigan R. D., 1981. Fixed Pitch Rotor Performance of Large Horizontal Axis Wind Turbines, Proceedings, *Workshop on Large Horizontal Axis Wind Turbines*, NASA CP-2230, DOE Publication CONF-810752, Cleveland, OH: NASA Lewis Research Center, pp. 69-85.
- Wilson, R. E., Lissaman, P. B. S., 1974. *Applied Aerodynamics of Wind Power Machines*, Oregon State University, Report N° NSF-RA-N-74-113.

## 8. RESPONSIBILITY NOTICE

The authors are the only responsible for the printed material included in this paper.